https://doi.org/10.1071/RD19068_AC
Supplementary Material: *Reproduction, Fertility and Development*, 2020, 32(5), 531–537

Supplementary material for

Betaine-loaded $CaCO_3$ microparticles improve survival of vitrified feline preantral follicles through higher mitochondrial activity and decreased reactive oxygen species

D. C. C. Brito[A,B,C,H], *S. F. S. Domingues*[B], *A. P. R. Rodrigues*[C], *L. M. Silva*[C], *K. A. Alves*[C], *X. Wu*[D,E], *T. S. Francisco*[F], *I. L. Barroso Neto*[F], *V. N. Freire*[F], *J. R. Figueiredo*[C], *J. C. Pieczarka*[A], *R. R. Santos*[B,G]

[A]Laboratory of Cytogenetics, Biological Sciences Institute, Federal University of Pará, Brazil.

[B]Laboratory of Wild Animal Biology and Medicine, Federal University of Pará, Brazil.

[C]Laboratory of Manipulation of Oocytes and Ovarian Pre-Antral Follicles (LAMOFOPA), Faculty of Veterinary Medicine, Ceará State University, Fortaleza, CE, Brazil.

[D]Hubert Department of Global Health, Rollins School of Public Health, Emory University, Atlanta, Georgia, United States of America.

[E]Department of Infectious Disease, Sir Run Run Shaw Hospital, College of Medicine, Zhejiang University, Hangzhou, P.R. China.

[F]Department of Physics, Federal University of Ceará, Brazil.

[G]Schothorst Feed Research, Lelystad, the Netherlands.

[Hs]Corresponding author. Email: daniellecalado@ymail.com

Figure S1. Representative images of fresh and vitrified feline ovarian tissues. A: fresh (non-vitrified); B: vitrified without betaine or ascorbic acid supplementation; C: vitrified in the presence of non-loaded 1 mM betaine; D: vitrified in the presence of 7.4 µM of betaine loaded $CaCO_3$ microparticles; E: vitrified in the presence of 74 µM of betaine loaded $CaCO_3$ microparticles; F: vitrified in the presence of non-loaded 0.3 mM ascorbic acid; G: vitrified in the presence of 20 µM of ascorbic acid loaded $CaCO_3$ microparticles; H: vitrified in the presence of 200 µM of ascorbic acid loaded $CaCO_3$ microparticles. Each bar represents 10 µm.

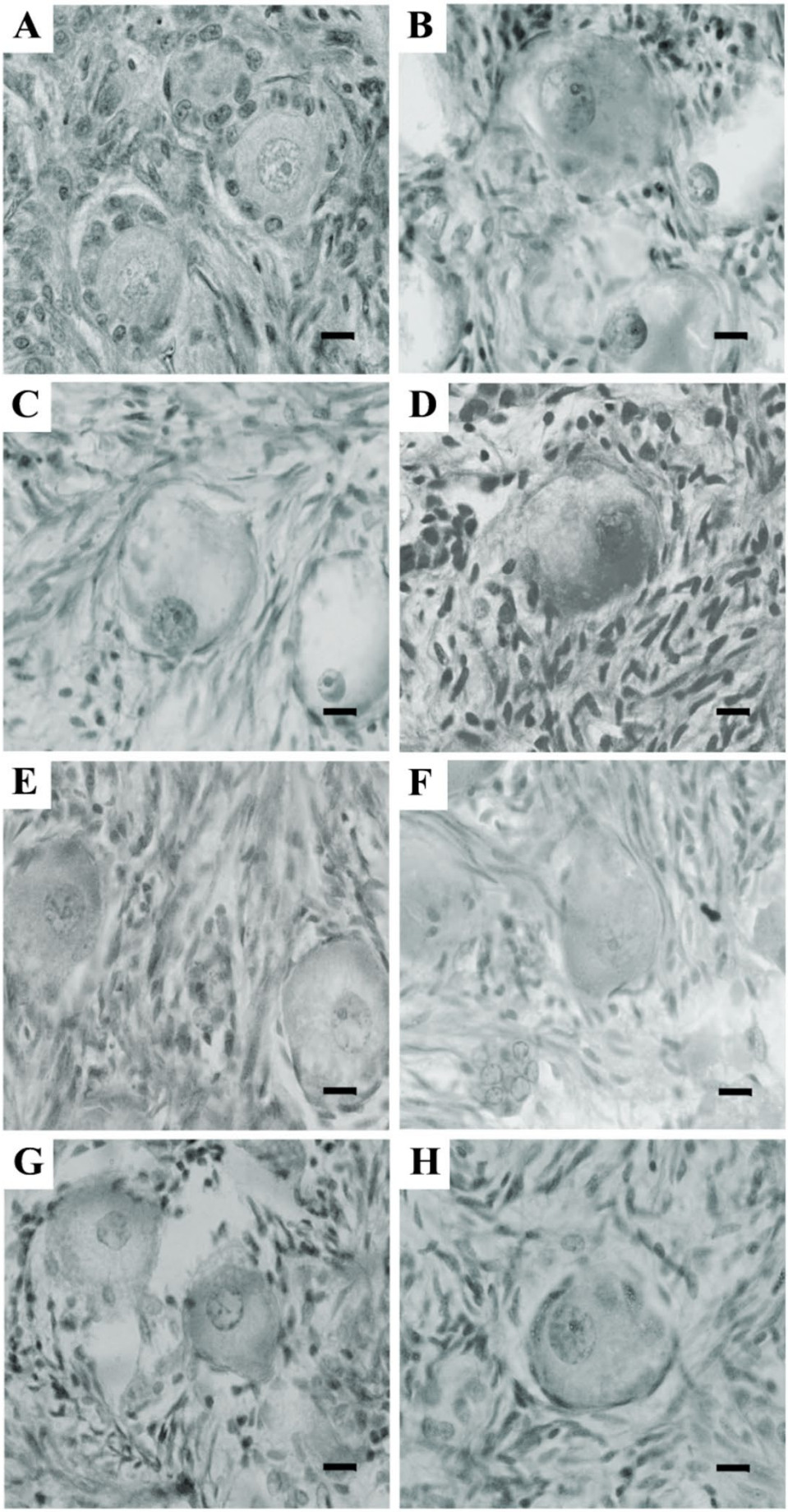
A
B
C
D
E
F
G
H

Figure S2. Violin plots detailing relative stromal cells density of vitrified ovarian tissue using fresh tissue as baseline. No significant differences were observed.

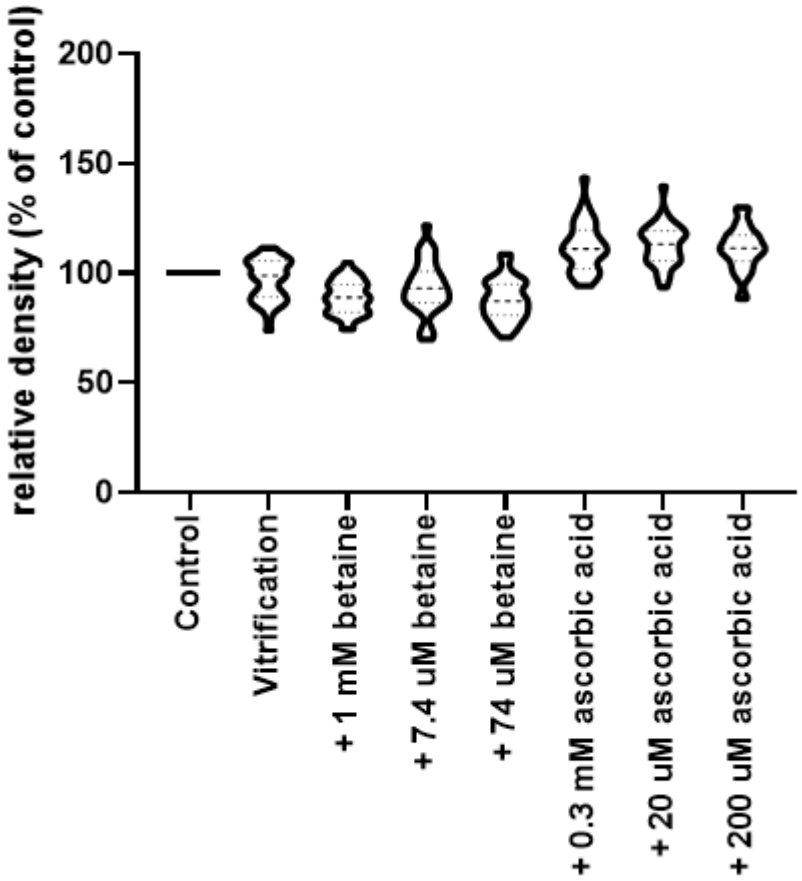

Table S1. Experimental protocol for the vitrification of ovarian fragments

N.A.: Not applicable

Vitrification solution	Intracellular cryoprotectants	Extracellular cryoprotectant	Supplement	Loading in $CaCO_3$ nanoparticle	Test compound	Concentration
No (control)	N.A.	N.A.	N.A.	N.A.	N.A.	N.A.
VS1	20% EG + 20% DMSO	0.1 M trehalose	No	N.A.	N.A.	N.A.
VS2	20% EG + 20% DMSO	0.1 M trehalose	Yes	No	Betaine	1 mM
VS3	20% EG + 20% DMSO	0.1 M trehalose	Yes	Yes	Betaine	7.4 μM
VS4	20% EG + 20% DMSO	0.1 M trehalose	Yes	Yes	Betaine	74 μM
VS5	20% EG + 20% DMSO	0.1 M trehalose	Yes	No	Ascorbic acid	0.3 mM
VS6	20% EG + 20% DMSO	0.1 M trehalose	Yes	Yes	Ascorbic acid	20 μM
VS7	20% EG + 20% DMSO	0.1 M trehalose	Yes	Yes	Ascorbic acid	200 μM

Supplementary materials and methods section

Choice of compounds and concentrations

With the aim to improve ovarian tissue and follicular quality during the vitrification process, two test compounds were selected. Among them, the use of antioxidant ascorbic acid (vitamin C) has been controversial. Melo *et al*. (2011) showed that supplementation of vitrification medium with 50 µg/ml (0.3 mM) enhanced the preservation of vitrified sheep primordial follicles, whereas Wiedemann *et al*. (2013) observed a detrimental effect on *in vitro* cultured feline ovarian tissue; however, Wiedemann et al. did not state the concentration of ascorbic acid that was used. Besides the oxidative stress, the use of an osmoprotector, more than only a sugar, may improve follicular preservation. Betaine is an organic osmolyte that occurs naturally in biological systems, playing a role in the protection of cells against osmotic stress (Lang 2011; Sokolov and Sokolova 2018). Moreover, it has been suggested that betaine serves as an efficient nontoxic cryoprotectant (Yang *et al*. 2016). Besides the presence of the antioxidants and osmoregulators in the medium, it is important to consider the tissue permeation with these compounds to avoid the use of inadequate concentrations, i.e. a suboptimal or excessive amount. For instance, ascorbic acid is only termed as an antioxidant. However, electrons from ascorbic acid can generate oxidants when it is used at millimolar concentrations (Parrow *et al*. 2013), whereas the minimum concentration expected in the plasma of a healthy human is 20 µM (Levine *et al*. 1996). Also, ascorbic acid is an anion at physiologic pH, which means that it will not diffuse across the cell membrane (Padayatty *et al*. 2016). Although much is known about ascorbic acid, there is a lack of information regarding *in vitro* tissue permeation with the osmolyte betaine. To allow the use of low concentrations of these compounds and improve their permeation in complex tissues, like ovarian tissues, the use of nano- or microcarriers is a prominent strategy. This might be possible with the help of $CaCO_3$ nano- or

microparticles. Compounds loaded in $CaCO_3$ have been reported to be more stable and retain a greater activity *in vitro* than when left in their free form (Wang *et al*. 2015; Ghafar *et al*. 2017).

Loading of betaine and ascorbic acid in nanoparticles

For the synthesis of nanoparticles, two solutions were prepared: the first was composed of 132.3 mg of calcium chloride dissolved in 40 mL distilled water, and the second was composed of 180 mg of cetrimonium bromide (CTAB) dissolved in 20 mL of distilled water. Thereafter, a solution composed of 10 mg betaine or ascorbic acid in 10 mL distilled water was added. The solutions were then heated to 50 °C on a hot plate coupled with magnetic stirring for four hours, resulting in an emulsion. Then, 99 mg sodium carbonate was dissolved in 100 mL distilled water and added to the solution at room temperature, with continuous stirring for one hour. Subsequently, the obtained nanoparticles were separated through filtration through paper (Fitec, Sao Paulo, SP, Brazil; ref no. 05P2392.08.CF) (Frazão *et al*. 2012).

Morphological characterisation of the nanomaterials - scanning electron microscopy

The particle size and morphology of the nanomaterial were analysed using scanning electron microscopy (SEM) FEG Quanta 450 ambiental with energy dispersive x-ray spectrometry and electron backscatter diffraction (EDS/EBSD (ThermoFisher Scientific, Waltham, MA, USA). For this, the nanoparticles were fixed in carbon tape and covered with gold particles. Subsequently, they were evaluated with SEM using a Quorum Q150T ES system (Quorum Technologies, Lewes, UK).

Adsorption simulations of betaine and ascorbic acid

The adsorption simulations of betaine and ascorbic acid molecules on the surface of the $CaCO_3$ nanoparticles were performed by molecular mechanics calculations. Simulation was performed at physiological pH (7.4). First, the systems (betaine or ascorbic acid loaded into $CaCO_3$ nanoparticles) were optimised using the classic Universal force field (UFF) (Rappé et

al. 1992). The resulting structures were subjected to a classical annealing calculation using the Forcite software from the Materials Studio suite. Each of the 100 annealing cycles were programmed with a minimum temperature of 200 K (–73.15ºC) and a maximum of 300 K (26.85ºC), with 50 heating ramps and 100 steps of 1 fs per ramp. For this calculation, the set was considered canonical (NVT), where the variables constant number (N), volume (V) and temperature (T) were conserved. The temperature control was performed with a Nosé thermostat. Structures obtained by this procedure were selected as inputs for calculations of the adsorption potential (Frazão *et al*. 2012).

The adsorption energy of each molecule on the surface of the $CaCO_3$ nanoparticle was defined as the energy difference between the total system (betaine or ascorbic acid loaded in $CaCO_3$ nanoparticles) and the energy of each component, which was calculated separately. An adsorption energy profile (distance versus potential energy) was evaluated for the selected structures (10 different local minimum energy points along the annealing cycles). The profile was obtained as a function of the centroid-centroid distance ($C\text{-}C_d$) in order to estimate the potential energy for betaine- and ascorbic acid-$CaCO_3$ complexes. The potentials were computed within the classical molecular mechanics formalism. The following convergence thresholds were adopted for the classical molecular mechanics computations: energy variation between two successive steps smaller than 2.0×10^{-5} kcal/mol, force per atom smaller than 0.001 kcal/mol/A, maximum displacement smaller than 1.0×10^{-5} A.

Vitrification of ovarian tissue

The ovarian tissue cryosystem (OTC) is a closed system; it was used as previously described (Carvalho *et al*. 2013). The fragments were exposed to the test vitrification solutions and vitrified according to Brito *et al*. (2018*b*). Briefly, the ovarian fragments were exposed to the different cryoprotectant solutions following a two-step concept, where the first exposure

was performed for 4 min at 20°C in vitrification solution 1 (VS1) and the second exposure was performed for 1 min at 20°C in VS2. Vitrification solutions were prepared with phenol red-free RPMI-1640 as the base medium and no serum was added. Exposure was performed into the OTC, which was closed and immediately immersed vertically in liquid nitrogen. After storage in liquid nitrogen (–196°C) for up to one week, OTCs containing the vitrified ovarian fragments were warmed by air at room temperature (RT ~25°C) for 1 min, followed by immersion in a water bath (37°C) for 30 sec. After warming, the cryoprotectants were removed by three-step washing solutions: (i) RPMI + 0.25 M trehalose (3 min), (ii) RPMI + 0.125 M trehalose (5 min), and (iii) RPMI (7 min). Vitrified-warmed ovarian fragments were submitted to histologic analysis, detection of reactive oxygen species and mitochondrial activity.

Histology

After fixation in Davidson solution (routine histology), ovarian fragments were dehydrated in ethanol, clarified with xylene and embedded in paraffin wax. Serial sections (5 μm) of ovarian tissue were cut and every fifth section was mounted on glass slides and stained with haematoxylin-eosin. All sections (20 sections/treatment per ovary) were examined using a light microscope (Leica) at a magnification of ×200. Primordial follicles were defined as those containing an oocyte surrounded by one flattened layer of granulosa cells, while developing preantral follicles contained an oocyte surrounded by at least one layer of cuboidal granulosa cells. To avoid counting a follicle more than once, primordial and developing preantral follicles were counted only in the sections where their oocyte nucleolus was observed. Follicular quality was evaluated based on the morphological integrity of the oocyte, the granulosa cells and the basement membrane. In brief, follicles were classified as normal (containing intact oocyte and well-organised granulosa cells without a pyknotic nucleus) or degenerated (containing a shrunken oocyte with a pyknotic nucleus, with normal or disorganised granulosa cells) (Lima *et al*. 2006).

The density of primordial and developing preantral follicles, per group or as total, was calculated as the total number of follicles, per class, divided by the total tissue volume and expressed as the number of follicles/mm^3 of ovarian tissue (Asadi-Azarbaijani *et al*. 2017). The volume of the analysed ovarian sections was calculated by summing the number of sections of area multiplied by the thickness of each section. The areas were measured by using Nikon's NIS-Elements software with ×4 magnification.

The ovarian stroma tissue histology images were transformed into RGB images and analyzed by image J 1.4.7 to quantify the average density of green, red, and blue. Automated on-line collection of ovarian stroma images was used to generate a surface plot image by Image J 1.4.7, which utilized a fire LUT (look up table) for colour presentation to estimate the ovarian tissue density.

Confocal laser scanning microscopy

Quantification of ROS and mitochondrial activity was performed using confocal laser scanning microscopy (CLSM; Leica TCS SPE-II, Mannheim, Germany), as previously described (Fabbri *et al*. 2016), with some modifications. In brief, the ovarian fragments were incubated for 30 min in the dark at 25°C with 0.2% MitoTracker Orange CMTMRos in phosphate buffer saline (PBS) for the detection of mitochondrial activity. Subsequently, the fragments were incubated for 30 min in the dark at 25°C with 0.1% 2′,7′-dichlorodihydrofluorescein diacetate (DCDHF DA, D6883; Sigma Aldrich, Oakville, Ontario) in PBS, which is oxidized by peroxides forming the DCF. The level of oxidative stress was measured by the fluorescence emission of DCF. After being labelled, fragments were washed three times in PBS, fixed in 4% paraformaldehyde for 15 min and stored in PBS at 4 °C until analysis using CLSM. Image generation was achieved using the 488 and 543 nm wavelengths for DCF and MitoTracker, respectively. For the quantification of ROS production and mitochondrial activity, a series of images in the *z* axis were obtained, followed by digitized

images in selected optical planes with an EZ-C1 Gold Version 3.70 software platform for the Nikon C1 (Nikon Instruments, NY, USA). Thereafter, the fluorescent intensity derived from the ovarian tissue was determined relative to the evaluated area, resulting in an arbitrary densitometric unit (ADU), as previously performed by Fabbri *et al*. (2016). All parameters that should interfere with fluorescence intensity, i.e. laser energy, signal detection (gain) and pinhole size, were kept at constant values during all measurements.

References

Asadi-Azarbaijani, B., Santos, R.R., Jahnukainen, K., Braber, S., van Duursen, M.B.M., Toppari, J., Saugstad, O.D., Nurmio, M., Oskam, I.C. (2017). Developmental effects of imatinib mesylate on follicle assembly and early activation of primordial follicle pool in postnatal rat ovary. *Reprod. Biol.* **17**, 25-33.

Brito, D.C.C., Domingues, S.F.S., Rodrigues, A.P.R., Figueiredo, J.R., Santos, R.R., Pieczarka, J.C. (2018*a*). Vitrification of domestic cat (*Felis catus*) ovarian tissue effects of three different sugars. *Cryobiology* **83**, 97-99.

Brito, D.C.C., Domingues, S.F.S., Rodrigues, A.P.R., Maside, C., Lunardi, F.O., Wu, X., Figueiredo, J.R., Pieczarka, J.C., Santos, R.R. (2018*b*). Cryopreservation of domestica cat (*Felis catus*) ovarian tissue comparison of two vitrification methods. *Theriogenology* **111**, 69-77.

Carvalho, A.A., Faustino, L.R., Silva, C.M., Castro, S.V., Lpes, C.A., Santos, R.R., Bao, S.N., Figueiredo, J.R., Rodrigues, A.P. (2013). Novel wide-capacity method for vitrification of caprine ovaries: ovarian tissue cryosystem (OTC). *Anim. Reprod. Sci.* **138**, 220-227.

Fabbri, R., Vicenti, R., Macciocca, M., Martino, N.A., Dell'Aquila, M.E., Pasquinelli, G., Morselli-Labate, A.M., Seracchioli, R., Paradisi, R. (2016) Morphological, ultrastructural and

functional imaging of frozen/thawed and vitrified/warmed human ovarian tissue retrieved from oncological patients. *Hum. Reprod.* **31,** 1838-1849.

Frazão, N.F., Albuquerque, E.L., Fulco, U.L., Azevedo, D.L., Mendonça, G.L.F., Lima-Neto, P., Caetano, E.W.S., Santana, J.V., Freire, V.N. (2012). Four-level levodopa adsorption on C60 fullerene for transdermal and oral administration: a computational study. *RSC Advances.* **2**, 22.

Ghafar, S.L.M.A., Hussein, M.Z., Rukayadi, Y., Zakaria, M.Z.A.B. (2017) Surface-functionalized cockle shell-based calcium carbonate aragonite polymorph as a drug nanocarrier. *Nanotechnol. Sci. Appl.* **10**, 79-94.

Lang, F. (2011) Effect of cell hydration on metabolism. *Nestle Nutr. Inst. Workshop. Ser.* **69**, 115-126.

Levine, M., Conry-Cantilena, C., Wang, Y., Welch, R.W., Washko, P.W., Dhariwal, K.R., Park, J.B., Lazarev, A., Graumlich, J.F., King, J., Cantilena, L.R. (1996) Vitamin C pharmacokinetics in healthy volunteers: evidence for a recommended dietary allowance. *Proc. Natl. Acad. Sci. USA* **93**. 3704–3709.

Lima, A.K, Silva, A.R., Santos, R.R., Sales, D.M., Evangelista, A.F., Figueiredo, J.R., Silva, L.D. (2006). Cryopreservation of preantral ovarian follicles in situ from domestic cats (Felis catus) using different cryoprotective agents. *Theriogenology* **66**, 1664-1666.

Melo, M.A., Oscam, I.C., Celestino, J.J., Carvalho, A.A., Castro, S.V., Figueiredo, J.R., Rodrigues, A.P., Santos, R.R. (2011) Adding ascorbic acid to vitrification and IVC medium influences preantral follicle morphology, but not viability. *Reprod. Domest. Anim.* **46**, 742-745.

Padayatty, S.J., Levine, M. (2016) Vitamin C physiology: the known and the unknown and Goldilocks. *Oral Dis*. **22**, 463-493.

Parrow, N.L., Leshin, J.A., Levine, M. (2013) Parenteral ascorbate as a cancer therapeutic: a reassessment based on pharmacokinetics. *Antioxid. Redox. Signal.* **19**, 2141–2156.

Rappe, A.K., Casewit, C.J., Colwell, K.S., Goddard, W.A., Skid, W.M. (1992) UFF, a full periodic table force field for molecular mechanics and molecular dynamics simulations. J. Am. Chem. SOC. 114, 10025.

Sokolov, E.P., Sokolova, I.M. (2018) Compatible osmolytes modulate mitochondrial function in a marine osmoconformer Crassostrea gigas (Thunberg, 1793). *Mitochonrdion* **17**, 30182-30184.

Wang, Y., Yamamoto, Y., Shigemori, S., Watanabe, T., Oshiro, K., Wang, X., Wang, P., Sato, T., Yonekura, S., Tanaka, S., Kitazawa, H., Shimosato, T. (2015) Inhibitory/suppressive oligodeoxynucleotide nanocapsules as simple oral delivery devices for preventing atopic dermatitis in mice. *Mol. Ther.* **23**, 297–309.

Wiedemann, C., Zahmel, J., Jewgenow, K. (2013) Short-term culture of ovarian cortex pieces to assess the cryopreservation outcome in wild felids for genome conservation. *BMC Vet. Res.* **9**, 37.

Yang, J., Cai, N., Zhai, H., Zhang, J., Zhu, Y., Zhang, L. (2016) Natural zwitterionic betaine enables cells to survive ultrarapid cryopreservation. *Sci. Rep.* **6**, 37458.